

Atrophy Analysis of Corpus Callosum in Alzheimer Brain MR Images Using Anisotropic Diffusion Filtering and Level sets

Anandh K R, Sujatha C M and Ramakrishnan S

Abstract—In this work, an attempt has been made to analyze the atrophy of Corpus Callosum (CC) in Alzheimer brain magnetic resonance images using anisotropic diffusion filtering and modified distance regularized level set method. Anisotropic diffusion filtering is used as preprocessing to obtain the edge map. The modified distance regularized level set method is employed to segment CC using this edge map. Geometric features are extracted from the segmented CC and are analyzed.

Results show that anisotropic diffusion filtering is able to extract the edge map with high contrast and continuous boundaries. Modified distance regularized level set method could perform the segmentation of CC in both normal and Alzheimer images. The extracted geometric features such as minor axis, euler number and solidity are able to demarcate the Alzheimer subjects from the control normals. As atrophy of CC is closely associated with the pathology, this study seems to be clinically useful.

I. INTRODUCTION

Alzheimer's Disease (AD) is a complex neurodegenerative disorder that causes memory impairment problems. AD results in atrophy changes of gray matter and white matter structures and thus leading to whole brain shrinkage. World Alzheimer report cites that approximately 35.6 million people around the globe lives with dementia. Since the origination of AD is still completely unknown there is no complete cure for this disease [1, 2, 3].

Corpus Callosum (CC) is the largest white matter structure which connects the left and right cerebral hemisphere. The reports on the study of CC reveal that its atrophy is closely associated with the progression of AD [4]. However, there exists large overlap in the volume of brain structures in the normal and AD subjects. Consequently, shape based analysis is adopted to demonstrate the disease pathology [5].

Magnetic Resonance (MR) imaging is a useful non-invasive imaging modality which reflects the brain pathology due to AD. Due to its high contrast and good resolution, it is widely preferred in brain related disorders than other imaging modalities. Moreover, it is capable of demonstrating the different stages of pathological conditions of AD [6].

Segmentation and feature extraction are essential in the study of atrophy analysis of CC [7]. Adaptive mean shift

clustering and geometric active contour models have been attempted to segment CC [8]. CC has also been segmented using deformable active Fourier contour model and rule based technique [9, 10]. There are reports that, the existing segmentation methods fail due to the substructure complexities and variations in the image parameters such as contrast, threshold, signal to noise ratio and inhomogeneity [11].

Level Set (LS) methods are dynamic curves or surfaces that undergo contour evolution to track complex topological changes. The reinitialization employed to maintain the stability during the evolution causes practical challenges and mathematical errors in the implementation of LS function [12]. The diffusion rate equation used in the regularization term can be modified to overcome the re-initialization problem [13].

In conventional LS method, Gaussian filtering is used to generate the edge map. However this introduces blurring and loses edge information. This often leads to either a premature or a delayed termination of the curve evolution process. Anisotropic diffusion is nonlinear diffusion filtering method which is employed as the pre-processing step for segmentation to generate edge map. This method reduces noise, preserve and highlights the edges [14].

In this work, the atrophy of corpus callosum in brain magnetic resonance images is analysed using anisotropic diffusion filtering and modified distance regularized level set method. The anisotropic diffusion filtering is employed as pre-processing to generate the edge map. The obtained edge indicator is used as edge stopping function in the modified distance regularized level set method to segment CC. Geometric features are extracted from the segmented CC and are normalized.

II. METHODOLOGY

A. Image Database

In this work, sagittal view T1 weighted brain MR images (Normal=20 and AD=20) are obtained from open access series of imaging studies, a public domain database. The images are acquired using 1.5-T vision scanner in a single imaging session [15].

B. Anisotropic Diffusion Filtering

Partial differential equations are used in the diffusion algorithms to remove noise by modifying the original or noisy image. Therefore, the linear isotropic diffusion equation with the initial condition $I(x, y, 0)$ is given by

$$\frac{\partial I(x,y,t)}{\partial t} = \text{div}(\nabla I) \quad (1)$$

Anandh K R is with the Anna University, Chennai 600025, India. (phone: +91-9443814369; e-mail: anandhmurali@gmail.com).

Sujatha C M, is with Anna University, Chennai 600025, India. (e-mail: sujathacm@annauniv.edu).

Ramakrishnan S is with the Department of Applied Mechanics, Indian Institute of Technology Madras, Chennai 600036, India. (e-mail: sramki@iitm.ac.in).

where $I(x, y)$ is the original image in the continuous domain with x, y as the spatial position, t indicates the artificial time parameter and ∇I is the image gradient. This produces the equivalent effect of filtering an image with a Gaussian filter (i.e) $I(x, y, t) = I_0(x, y) * G(x, y; t)$ where $I_0(x, y)$ is the original image and $G(x, y; t)$ is the Gaussian kernel of variance t . For larger value of t , more images can be derived at coarser resolution. Therefore, the linear type isotropic diffusion filtering (Gaussian filtering) causes blurring in the image.

To perform region specific smoothing and to overcome blurring at the edges, the classical isotropic diffusion is replaced by non-linear anisotropic diffusion equation and is given by

$$\frac{\partial I(x, y, t)}{\partial t} = \text{div}[f(\|\nabla I\|)\nabla I] \quad (2)$$

where $\|\nabla I\|$ is the gradient magnitude and $g(\|\nabla I\|)$ is the edge stopping function and is given by

$$f(\|\nabla I\|) = \exp\left(-\left(\frac{\|\nabla I\|}{k}\right)^2\right) \quad (3)$$

where k is the edge strength threshold. The diffusion gets stopped across the edges by letting $g(x) \rightarrow 0$ when $x \rightarrow \infty$. Let I_t be the filtered image obtained using non-linear anisotropic diffusion filter. The edge map 'g' can be extracted as given below

$$g = \frac{1}{1 + |\nabla I_t|^2} \quad (4)$$

C. Modified Distance Regularized Level Set Method

The basic level set evolution equation is given by

$$\frac{\partial C(t)}{\partial t} = \beta \vec{N} \quad (5)$$

where β is the speed function that influences the evolution speed, $C(t)$ can be expressed as a zero level set function $C(t) = \{(x, y) | \varphi(x, y, t) = 0\}$ and $\vec{N} = -\frac{\nabla \varphi}{|\nabla \varphi|}$ is the inward normal vector of $C(t)$. During the evolution, the level set function undergoes irregularities and loses stability. To avoid the re-initialization problem, Li proposed distance regularized levelset evolution. Unfortunately, it also faces stability problems in regularizing the level set function in some locations and the level set evolution becomes too flat. An improved diffusion rate equation is adopted to overcome this challenge. This rate equation is given by

$$d_p(|\nabla \varphi|) = \begin{cases} \frac{2}{\pi} \arctan\left(\frac{|\nabla \varphi| - 1}{\sigma}\right), & |\varphi| < \varepsilon \\ \frac{2}{\pi} \arctan\left(\frac{|\nabla \varphi| - 1}{\sigma}\right), & |\varphi| \geq \varepsilon \end{cases} \quad (6)$$

where, ε and σ are positive constant. By incorporating this improved diffusion rate equation in the variational energy minimisation level set framework, the level set evolution equation can be given as

$$\frac{\partial \phi}{\partial t} = \mu \text{div}(d_p(|\nabla \phi|)\nabla \phi) + \lambda \delta_\nu(\phi) \text{div}\left(g \frac{\nabla \phi}{|\nabla \phi|}\right) + \alpha g \delta_\nu(\phi) \quad (7)$$

where, $\mu > 0$ and $\lambda > 0$ are constants, δ_ν is the dirac function, α is the variable that controls the speed of the dynamic contour and g is the edge indicator obtained using eq.4. Geometric features are extracted from the segmented

CC and are normalized. Major axis shows the object elongation between two points in ROI. The minor axis is

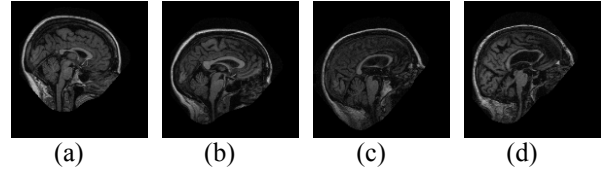


Figure 1. Representative set of original (a-b) Normal and (c-d) AD images

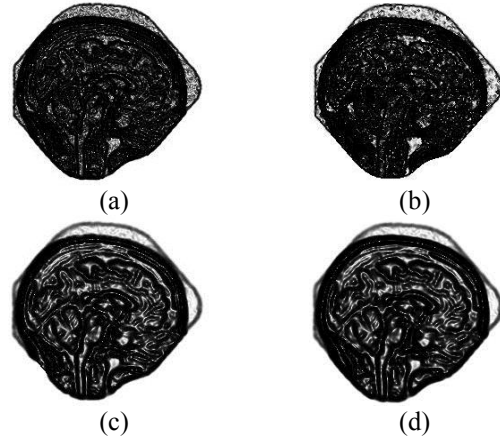


Figure 2. Extracted edge maps of (a) Gaussian filter and Anisotropic diffusion filtering for (b) k=5 (c) k=50 (d) k=490

drawn perpendicular to the major axis where the line has maximum length. Euler number with 8 connectivity concept gives the object number in the segmented region minus number of holes in the same region. Solidity is given by the proportion of pixels in the segmented region and also present in the convex hull.

III. RESULTS AND DISCUSSION

A representative set of normal brain MR and AD images in the sagittal view is shown in Fig.1. It is seen that, CC has different size and orientation in both normal and AD images. Although it has definite boundary, it is found to have varying length in both the normal and AD conditions. These images are subjected to non-linear anisotropic diffusion filtering to extract the edge map. Anisotropic diffusion filter with 5 iteration is employed to enhance the edge extraction in all the images. Fig. 1 (b-d) shows the edge maps obtained using this filter for different values of Gradient modulus threshold (k). The whole diffusion process undergoes 5 iterations to perform region specific smoothing. It is also observed that the edge maps generated with $k=5$ and 50 do not yield clear edges. In this work, k is empirically fixed a 490 to generate continuous and high contrast edges in all the images.

Conversely, edge map generated using traditional linear Gaussian filter is shown to have unclear boundaries in Fig. 2(a). Therefore, level set function would find it difficult in extracting the regions and might result in leakage of contours. Further, the images are subjected to modified distance regularized level set method to segment CC. The initial

contours of this region continuously evolve for every iteration by shrinking towards the edge map.

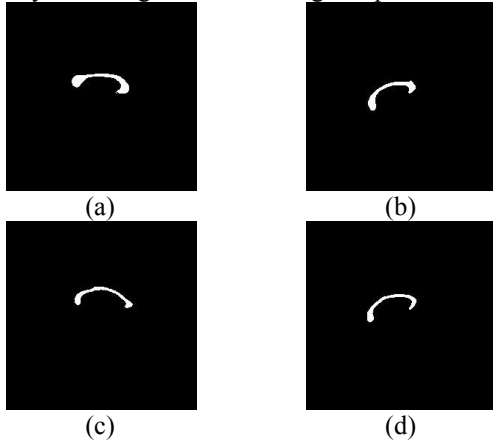


Figure 3. Segmented CC of (a-b) Normal and (c-d) AD images using edge maps of anisotropic diffusion filter

During the LS evolution, the contour speed parameter α controls the motion of level set function towards the desired region of interest. Weak edges of CC would require low value of α and more number of iterations. On the contrary, high value of α with low number of iteration can be used for strong and larger edges to privilege speedy evolution. In this study, α is chosen at 0.3 since both the CC is found to have small boundaries.

TABLE I. ANALYSIS OF THE GEOMETRIC FEATURES OF CC

Geometric features	Normal	Alzheimer's Disease
	Mean \pm SD	Mean \pm SD
Minor axis	0.77 \pm 0.10	0.70 \pm 0.11
Euler No	0.78 \pm 0.13	0.73 \pm 0.15
Solidity	0.67 \pm 0.15	0.63 \pm 0.12

SD-Standard Deviation

The level set function took 15 iterations to extract CC in all the normal and AD images. Fig. 3 shows the segmented images of CC. A slight change of tissue loss in the segmented CC is observed in AD images compared to the normals. Shape based geometric features are extracted from the segmented CC and are normalized. Analysis of the geometric features of CC is shown in Table 1. The features such as minor axis, euler number and solidity has difference in the magnitude values of mean and Standard Deviation (SD) for the normal and AD images.

To graphically demonstrate the pathology of AD, box plot are plotted for these features in Fig. 4 (a-c). It is observed that the features namely minor axis and euler number shows higher discrimination between normal and AD subjects than solidity. This might be due to the reduction of thickness of CC tissue in the AD condition. Solidity shows only a small difference in the mean values and this might be attributed to the slight variation in the reduction of area in AD subjects compared to control normals.

To further differentiate the tissue loss, percentage of difference of mean value has been calculated for the features and is displayed in Fig. 5. The features minor axis and euler

number shows appreciable difference in their mean values compared to solidity. Minor axis and euler number has percentage difference of 9.52 and 6.62 respectively, while solidity shows 6.15 percent difference.

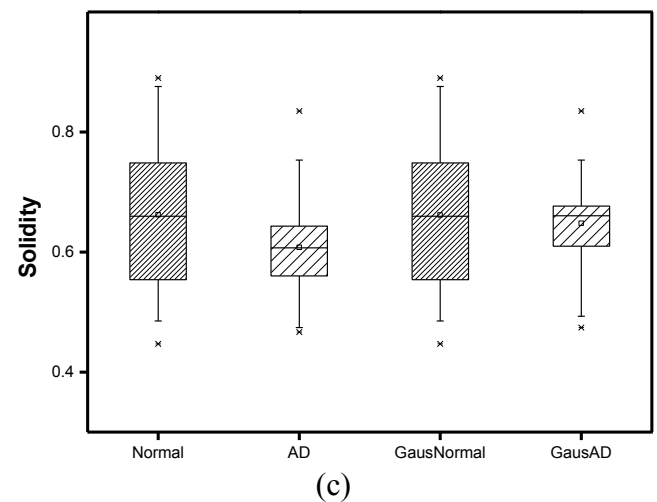
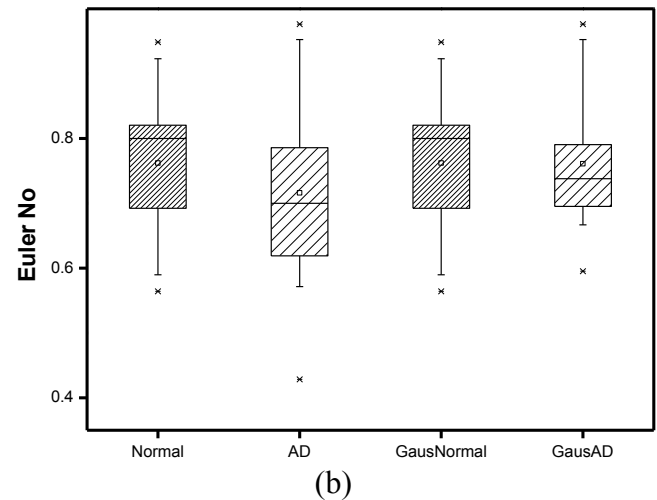
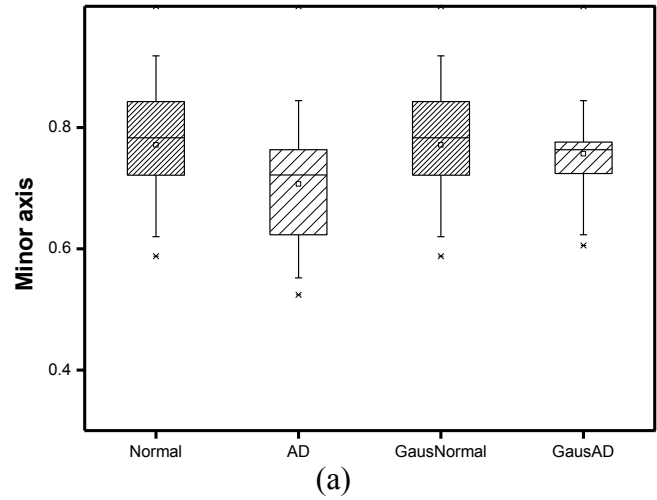


Figure 4. Variations in the geometric features of segmented CC images (a) Major axis (b) Minor axis and (c) Euler number using edge maps of anisotropic diffusion filter

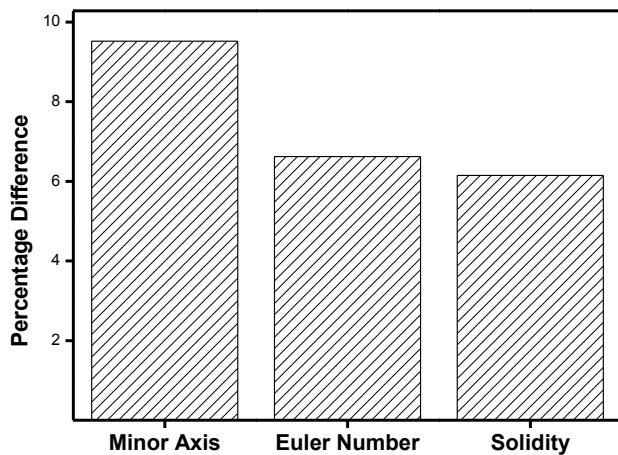


Figure 5. Bar plot representing the percentage difference between normal and AD subjects using edge maps of anisotropic diffusion filter

IV. CONCLUSION

AD is a complex brain related disorder that causes cognitive deficits such as memory loss and difficulties in performing daily activities. It also causes atrophy in gray matter and white matter structures thereby leading to nerve cell deaths. Callosal reduction is a significant biomarkers for the diagnosis of AD. Segmentation and shape analysis are essential for the characterization of the disease. Robust edge extraction is required to precisely segment the substructure.

The edge map extracted using Gaussian diffusion appears to be blurred. Nonlinear anisotropic diffusion filtering is performed on the images to generate edge map with sharp boundaries. This edge map is used as the edge stopping function in the modified distance regularized level set method. Geometric features are extracted from the segmented CC and normalized.

Results show that anisotropic diffusion filtering is able to preserve and sharpen the edges in both the normal and AD images through region specific smoothing. The modified distance regularized level set method extracts CC in normal and AD images. The geometric features of CC show clear demarcation in the AD subjects. Thus this study seems to be clinically useful in quantifying the atrophy of CC due to the pathology.

ACKNOWLEDGMENT

Sincere acknowledgements to Anna University, Chennai.

REFERENCES

[1] N. M Sean, R. Rupsingh, M. Borrie, M. Smith, V. Accomazzi, J. L. Wells et al., "Ventricular enlargement as a possible measure of Alzheimer's disease progression validated using the Alzheimer's disease neuroimaging initiative database," *Brain*, vol. 131, pp. 2443-2454, 2008.

[2] M. W. Weiner, D. P Veitch, P. S. Aisen, L. A. Beckett, N. J. Cairns, R. C. Green et al "The Alzheimer's Disease Neuroimaging Initiative:

a review of papers published since its inception," *Alzheimer's & Dementia*, vol. 8, pp. 1-68, 2012.

[3] S. M. Nestor, R. Rupsingh, M. Borrie, M. Smith, V. Accomazzi, J. L. Wells et al "Alzheimer's Disease Neuroimaging Initiative. Ventricular enlargement as a possible measure of Alzheimer's disease progression validated using the Alzheimer's disease neuroimaging initiative database," *Brain*, vol. 131, pp. 2443-54, 2008.

[4] M. Di Paola, G. Spalletta and C. Caltagirone, "In Vivo Structural Neuroanatomy of Corpus Callosum in Alzheimer's Disease and Mild Cognitive Impairment Using Different MRI Techniques: A Review," *Journal of Alzheimer's Disease*, vol. 20, pp. 67-95, 2010.

[5] L. Ferrarini, M. P. Walter, O. Hans, A. B. Mark et al, "Shape differences of the brain ventricles in Alzheimer's disease," *NeuroImage*, vol. 32, pp. 1060-1069, 2006.

[6] B. S. Mahanand, S. Suresh, N. Sundararajan and M. A. Kumar, "Identification of brain regions responsible for Alzheimer's disease using a Self-adaptive Resource Allocation Network," *Neural Networks*, vol. 32, pp. 313-322, 2012.

[7] R. Chaves, J. M. Górriz, C. G. Puntinet and J. Ramirez, "Alzheimer's Disease Neuroimaging Initiative. Association rule-based feature selection method for Alzheimer's disease diagnosis," *Exp Sys App*, vol. 39, pp. 11766-11774, 2012.

[8] L. Yue, M. Mrinal, S. N. Ahmed, "Fully Automated Segmentation of Corpus Callosum in Midsagittal Brain MRIs," in *Proc. 35th Int. Conf. on IEEE EMBS*, Osaka, Japan, July, 2013.

[9] C. Vachet, B. Yvernault, K. Bhatt and R. G. Smith, "Automatic corpus callosum segmentation using a deformable active Fourier contour model," *Proc. Soc Photo Opt Instrum Eng*. 2012.

[10] T. J. Herron, X. Kang and D. Woods, "Automated measurement of the human corpus callosum using MRI," *Frontiers in neuroinformatics*, vol. 6, pp. 1-15, 2012.

[11] S. Ralf, P. David, R. J. Anna et al, "Automated segmentation of lateral ventricles from human and primate magnetic resonance images using cognition network technology," *Mag Res Img*, vol. 24, pp. 1377-1387, 2006.

[12] C. Li, C. Xu, C. Gui et al, "Distance regularized level set evolution and its application to image segmentation," *IEEE Trans. Image Process*, vol. 19, pp. 154-164, 2010.

[13] W. Wu, Y. Wu and Q. Huang, "An improved distance regularized level set evolution without re-initialization," in *Proc. Fourth Int. Conf on Advan Comput Intell*, pp. 631, Oct 2012.

[14] P. Perona and J. Malik, "Scale-Space And Edge Detection Using Anisotropic Diffusion," *IEEE Trans. Pattern Anal. Mach. Intell*, vol. 12, pp. 629-639, 1990.

[15] D. S. Marcus, T. H. Wang, J. Parker et al, "Open Access Series of Imaging Studies (OASIS): cross-sectional MRI data in young, middle aged, nondemented, and demented older adults," *J Cognitive Neurosci*, vol. 19, pp. 1498-1507, 2007.